ADVANCED ENGINEERING MATERIALS

DOI: 10.1002/adem.200900192

Stress-Dependent Elastic Properties of Porous Microcracked Ceramics**

By *Irina Pozdnyakova, Giovanni Bruno*, Alexander M. Efremov, Bjørn Clausen* and *Darren Hughes*

Although ceramics are considered linear elastic materials, we have observed a non-linear pseudo-elastic behavior in porous cellular microcracked ceramics such as β-eucryptite. This is attributed to the evolution of microstructure in these materials. This behavior is particularly different from that of non-microcracked ceramics such as silicon carbide. It is shown that in microcracked materials two processes, namely stiffening and softening, always compete when a compressive external load is applied. The first regime is attributed to microcrack closure, and the second to microcracks opening, i.e. to a damage introduced by the applied stress. On the other hand rather a continuous damage is observed in the non-microcracked case. A comparison has been done between the microscopic (as measured by neutron diffraction) and the macroscopic stress-strain response. Also, it has been found that at constant load a significant strain relaxation occurs, which has two timescales, possibly driven by the two phenomena quoted above. Indeed, no such relaxation is observed for non-microcracked SiC. Implications of these findings are discussed.

In structural applications of ceramic materials, elastic properties are commonly required in product specifications as well as in computer simulations of a product behavior under variable conditions of stress and temperature. Usually, industrial ceramics are considered linear elastic materials. However, some inorganic compounds are already known to exhibit a dependence of elastic properties from applied stresses. For example, porous rocks often have elastic moduli which are not constant but increase with increasing stress.[1] In ref. [1] it was stated that the use of classical linear elasticity (i.e., constant modulus) can lead to erroneous predictions of the deformations and of the initiation and extent of failure around underground excavations. Moreover, it was found that Young's, shear and bulk moduli of a soil depend on the stress state, and a model for those dependencies was developed.[2] A recent work on ferroelectric ceramics has shown that the elastic response in these materials is nonlinear, and the reason for that is the ferroelastic domain switching.[3] Another extremely relevant work in this context is that of Heap *et al*.[4] These authors have found a variation of both Young's modulus and Poisson's ratio of basalt rocks as a function of cycle number in alternate loading. The explanation

[*] *Dr. G. Bruno*
Corning SAS, CETC
7bis Av.de Valvins, BP3, F-77210 Avon, France
E-mail: brunog@corning.com
Dr. I. Pozdnyakova
CEMHTI-CNRS
1d Av. De la Recherche Scientifique, 45071 Orleans Cedex 02, France
Dr. A. M. Efremov
Corning OOO, CSC
26 liter A, Shatelena Ulitsa, 194021 St. Petersburg, Russia
Dr. B. Clausen
LANSCE, LANL
1619 Central Avenue, MS A117, Los Alamos, NM 87545, USA
Dr. D. J. Hughes
ILL
6, rue Jules Horowitz 38042 Grenoble Cedex 9, France

[**] *James E. Webb (Corning Inc., CS&S, SP, NY, USA) Thomas A. Sisneros and Donald W. Brown (LANL, NM, USA) where members of the experimental team and are acknowledged for their help and for useful advices and discussions. James E. Webb and Lisa Noni (Corning Inc. SP, NY, USA) provided and characterized the β-eucryptite sample (MOR, Porosity, CTE, etc.– not reported), Thomas Glasson (Corning SAS, CETC, Avon, France) provided the SiC sample. This work has benefited from the use of the Lujan Neutron Scattering Center at LANSCE, which is funded by the Office of Basic Energy Sciences (DOE). Los Alamos National Laboratory is operated by Los Alamos National Security LLC under DOE Contract DE AC52 06NA25396. Beamtime on SALSA was kindly allocated by the ILL.*

COMMUNICATION

they gave is related to damage and microcracking. Interestingly, they found by acoustic emission (AE), that events can be recorded only if the load in a particular cycle exceeds any of the loads applied in previous cycle. They also found a nonlinear stress–strain behavior in each of the stress–strain cycles but did not go into details of this.

To describe the observed phenomenology, several models have been proposed.[2,5,6] These models explain well experimental results for particular samples and try to develop a general approach, but since the real physical processes involved are very complex, no microscopic mechanisms, which encompasses these phenomena was proposed. In addition, the experimental data available concern only specific class of materials—rocks and soils, whereas no attention, to the best of our knowledge, was paid to elastic behavior of industrial ceramics, with exception of work.[3]

Industrial ceramics generally have a complex microstructure. Even in the case where the ceramics are single-phased, they can be porous, and further, if there is a mismatch between coefficients of thermal expansion for different crystal axes, microcracks are inevitably created and, in turn, they influence elastic properties. In addition, to tailor ceramics to specific applications, new parameters are added, as for example the cellular structure. The latter is used for ceramic membranes and filters and can influence the mechanical properties of the ceramics as well.

The ceramics resistance to fracture and to applied stress has been investigated extensively, but little attention has been given to the elastic properties under load. Indeed, the best practice to measure the Young's modulus of those materials is given in an ASTM standard,[7] and it consists of the use of sonic resonance (SR) devices.[8] This is a load-free method and therefore is equivalent to measuring the slope of the stress–strain curve at zero load and deformation. Thus it assumes that the curve is linear. Under limited circumstances this method gives an approximation of the materials response in operating conditions of mechanical and/or thermal stress; however, the stress–strain curves can be nonlinear in porous and in microcracked ceramics, especially at high temperatures. This leaves a gap in the characterization of the mechanical response of ceramics and consequently in the assessment of their performance.

To the best of our knowledge, there are no studies concerning elastic response of functional ceramic materials upon external load and no works concerning the comparison of elastic behavior between industrial ceramics with different type of microstructure, namely, between solely porous and porous plus microcracked materials. Here, we report the results of macroscopic and microscopic stress–strain measurements for two porous cellular ceramics used for gas filtering and liquid separation membranes. We will see that new constitutive laws must be defined for microcracked materials, and that time becomes an important variable, especially in stress modeling from mechanical data.

Experimental

The materials under investigation were β-eucryptite and silicon carbide cellular porous ceramics. The samples were cut from larger specimens (2–6 inches in diameter) to a rectangular prism shape of about $12 \times 25 \times 50\,mm^3$, paying attention at always including whole cell walls as borders. The β-eucryptite sample underwent in situ neutron diffraction experiments, using an Instron test rig (with 10 kN load cell) in compression mode. The rig was mounted on the diffractometer Spectrometer for Materials Research at Temperature and Stress (SMARTS [9]) at the Los Alamos Neutron Science Center (Los Alamos, NM, USA). The measurements on SiC were carried out also on an Instron machine, with a 50 kN load cell, mounted on the instrument Strain Analyser for Large Scale engineering Applications (SALSA) (see refs. [10,11]) at the Institut Laue-Langevin, Grenoble, France. In parallel to neutron data acquisition, the macroscopic stress–strain curves were taken, using an extensometer (provided with the rig). A photo of the set-up on SMARTS is given in Figure 1(a). Special steel or aluminum platens (on SMARTS or SALSA, respectively) were built for the experiments.

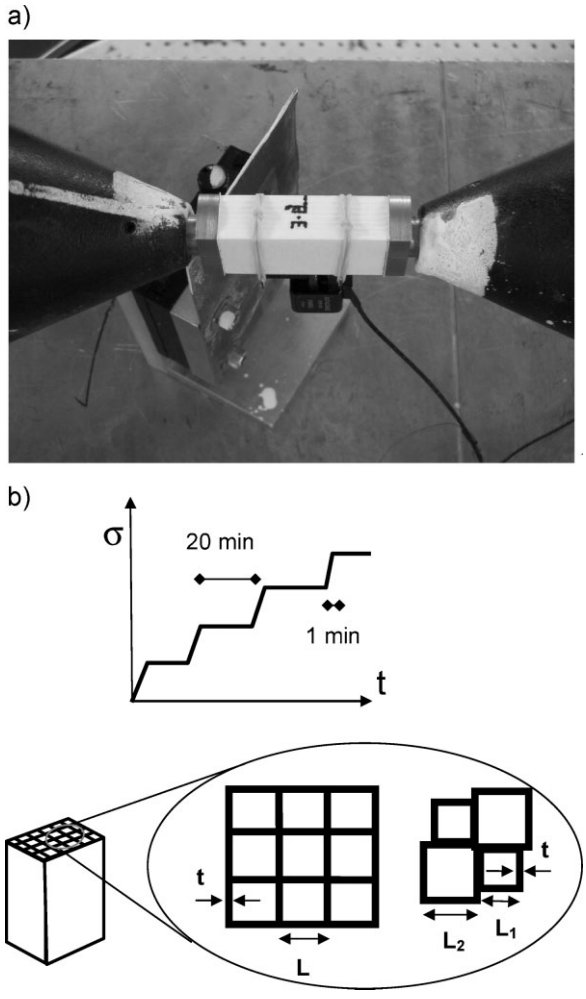

Fig. 1. (a) The β-eucryptite cellular sample, as mounted on the stress rig installed on SMARTS. Special steel platens have been built. The extensometer, attached with rubber bands, is visible on the bottom. (b) The time protocol typically used for all samples. The hold time could vary. (c) Scheme of the cell geometry for the symmetric β-eucryptite and the asymmetric SiC cellular specimens.

ADVANCED ENGINEERING MATERIALS

Table 1. Geometrical and physical properties of the investigated materials.

Material	t [mm]	L_1 [mm]	L_2 [mm]	$1/A_0$	MOR [MPa]	p
SiC	0.40	1.60	2.35	0.375	268.2	0.38
β-eucryptite	0.25	1.90	–	0.246	–	0.5

The applied stress value has been calculated reducing the total cross-section by the so-called open frontal area (i.e., taking into account the cellular geometry) according to the formulae [12]:

$$\sigma_{corr} = \sigma \times A_0 \quad (1)$$

where

$$A_0 = \left(\frac{t(2L-t)}{L^2}\right)^{-1} \text{ for symmetric cell configuration;}$$

$$A_0 = \left[\frac{1}{2}\left(\frac{t(2L_1-t)}{L_1^2} + \frac{t(2L_2-t)}{L_2^2}\right)\right]^{-1} \text{ for asymmetric cell configuration}$$

A schematic of the cross-section with the definition of the dimensions is given in Figure 1(c). The relevant geometrical and physical properties of those materials are listed in Table 1.

For the β-eucryptite sample (on SMARTS) the neutron counting time was about 20 min, so the sample was exposed for the same amount of time to a constant load. The stress–strain curves were measured in stress-controlled mode, whereby the stress profile versus time had a ladder-like shape: load ramps of about 0.1 kN min^{-1} were followed by 20 min long load holds. The actual hold time depended on the stability of the beam, and sometimes longer times were needed. The stress protocol as a function of time is shown in Figure 1(b).

Since SMARTS is a time-of-flight instrument, the whole diffraction spectrum in the range 0.8–3.8 Å is available, and therefore the unit cell lattice parameters are refinable by a Rietveld procedure. For the latter, the GSAS program was used [13]. Similar conditions applied for the SiC experiment on SALSA: a load rate of 1–2 kN min^{-1} has been used and diffraction spectra were acquired at fixed load for a time of about 5 min. For steady sources instruments like SALSA, usually, only one peak at a time is measured, but possibly two or three can be caught in the case if a position sensitive detector (PSD) is available. The neutron wavelength was $\lambda = 1.549$ Å; and for SiC, the hexagonal 116 and 203 peaks were measured, the first superposing to the cubic 311 peak.

The strain was calculated, as usual, as the relative lattice parameter (or interplanar distance) difference to the initial state (zero applied load).

From the slope of the applied stress versus macroscopic strain curves in each ramp segment, the Young's modulus was calculated by linear approximation. This treatment allowed determining the dependence of the Young's modulus on the applied stress. Also the total deformation under each constant load was tracked, as well as the dependence of the deformation change on exposure time.

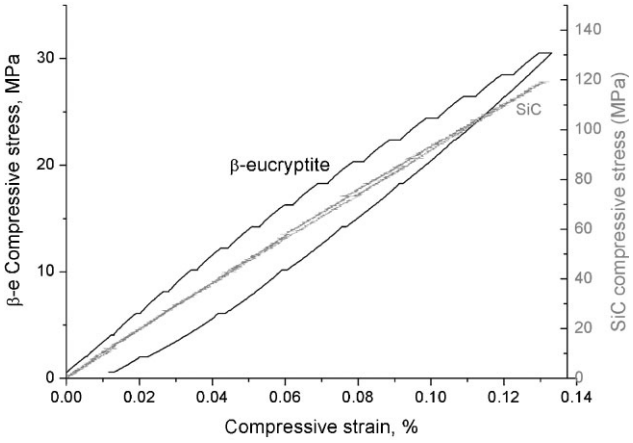

Fig. 2. Examples of the macroscopic stress–strain curves, as recorded throughout the whole ND experiments on β-eucryptite (in black) and SiC (in gray).

Results

The room temperature stress–strain curves for two samples are shown in Figure 2. For SiC the curve seems to be monotonic, whereas for β-eucryptite the curve shows specific ''ladder'' shape. For both materials, each of the ramp segments in Figure 2 can be well approximated by a straight line.

From this graph, it can be seen that the slopes are different from segment to segment, especially for β-eucryptite. Interestingly, the curvature of the stress–strain curves for β-eucryptite is different: upon loading, it is convex; upon unloading, it seems to be concave.

The corresponding lattice responses to the external applied stress are shown in Figure 3 for β-eucryptite and SiC, respectively. For β-eucryptite the two phases β-eucryptite and lithium aluminum oxide are shown. From the macroscopic stress versus microscopic strain data of Figure 3(a) it is clear that two roughly linear regimes can be identified for β-eucryptite, although some scatter is present, especially for the c-axis. This axis is supposed to be the most prone to microcracking, and therefore its sensitivity to the external applied stress is variable. For SiC both peaks show similar features of the stress–strain behavior: they have very similar slopes and show some hysteresis, thus at very high load relaxing the lattice strain.

We have to bear in mind that the strain at zero applied stress has been taken as reference. This discards the effect of any possible residual microstress, especially in β-eucryptite, due to thermal expansion mismatch between the crystal axes or between the two phases.

Data Interpretation

Young's Modulus

As mentioned before, the Young's modulus is a material property that describes the materials stiffness and is used in

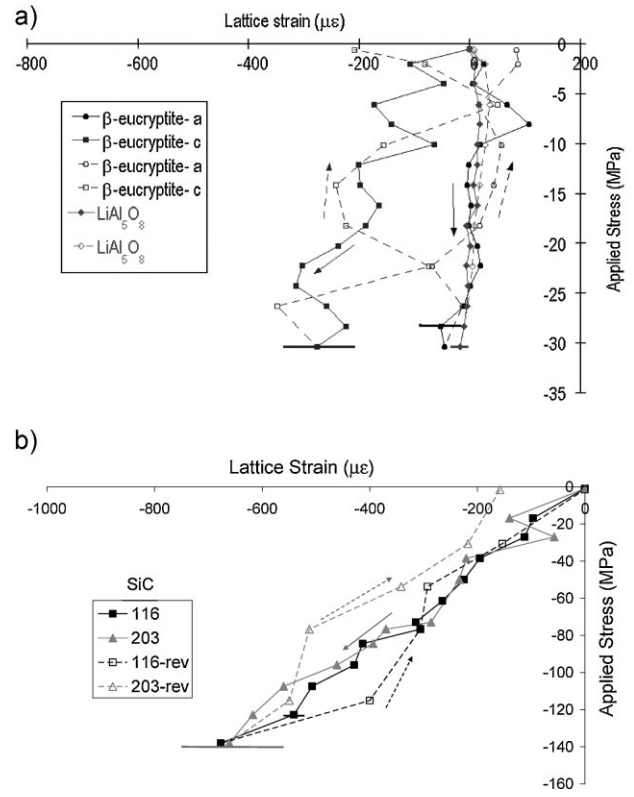

Fig.3. The microscopic stress–strain behavior of the materials investigated: (a) β-eucryptite and (b) SiC. Lattice strain units are given in με (ppm). Typical error bars (from the fitting procedure) are indicated by the bold horizontal lines.

different parameters that are directly related to the product durability, like the thermal shock resistance.[14] Usually, the Young's modulus is determined as the slope of stress–strain curve in the elastic regime. Thus, it is defined to be independent from the applied stress, although sometimes it is not the case.

A linear fit to individual segments of the strain–stress curves of Figure 2 was made, resulting in the dependence of the Young's modulus, E, versus applied stress, σ. The E versus σ dependencies for β-eucryptite and SiC during load and unload are shown in Figure 4. Since at low loads the imperfect extensometer mount can provide spurious results, the points obtained from the first and last ramps are omitted. It is seen that for SiC there is a decline of E upon loading of about 20%, whereas during unloading it is stable. For β-eucryptite the situation is more complex: upon loading, the curve $E(\sigma)$ possesses a local maximum, while during unloading it reaches a minimum. They are located at about the same stress value.

The phenomena driving the two different behaviors are linked to the microstructure of the materials: SiC is non-microcracked and therefore is simply prone to damage and pore re-shaping during loading, which leads to a steadily decreasing Young's modulus with increasing applied load. Upon unloading, the value stays constant, since this damage is irreversible. It must be noted that the unload rate was the double of the load rate for SiC and 1.5 times for β-eucryptite,

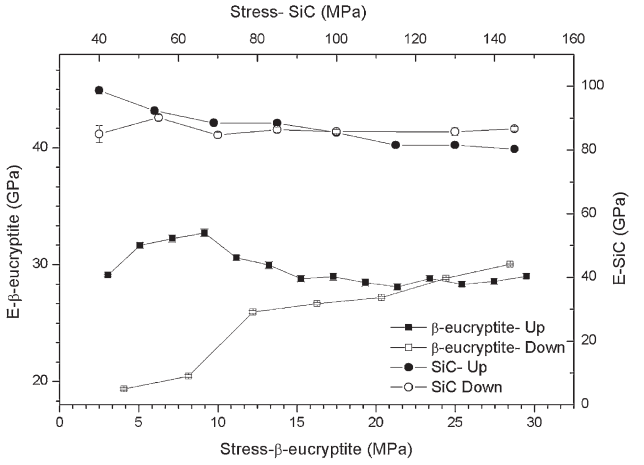

Fig. 4. The behavior of E as a function of the applied stress for β-eucryptite and SiC. Error bars are basically included in the symbols.

so that the small difference between the hollow and the full symbols (for both materials) is most probably due to the effect of the load rate.[15]

Apparent Creep Behavior

One of the most striking features that we can see in Figure 2 is that at each constant load level the β-eucryptite sample creeps, i.e., the compressive strain increases without increasing the applied stress. The situation is reverted upon unloading: the strain changes in the tensile direction, i.e., it follows the unloading. In order to estimate the effect of the applied stress on the sample deformation at constant load, the difference between the deformation at the beginning and at the end of each plateau was calculated (corresponding to the neutron diffraction acquisitions and taking always the same exposure time elapsed). This is shown in Figure 5. Interestingly, there are no such changes observed for SiC, possibly because of the insufficient exposure time under stress (5 min vs. 20 min for β-eucryptite). Although the deformation dynamics itself can be slower in SiC, most of the creep

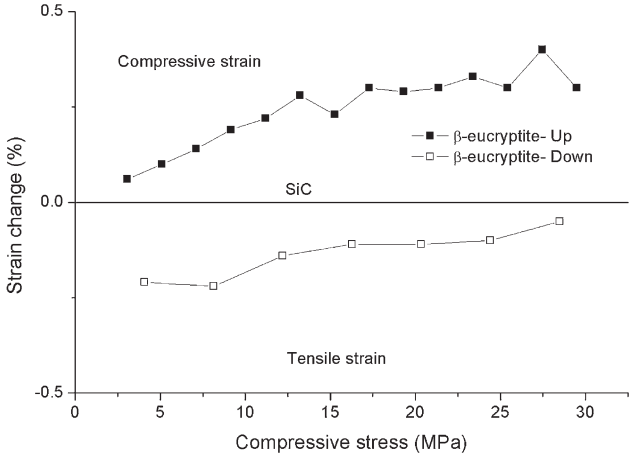

Fig. 5. The behavior of the strain change at constant stress as a function of the applied stress for β-eucryptite.

ADVANCED ENGINEERING MATERIALS

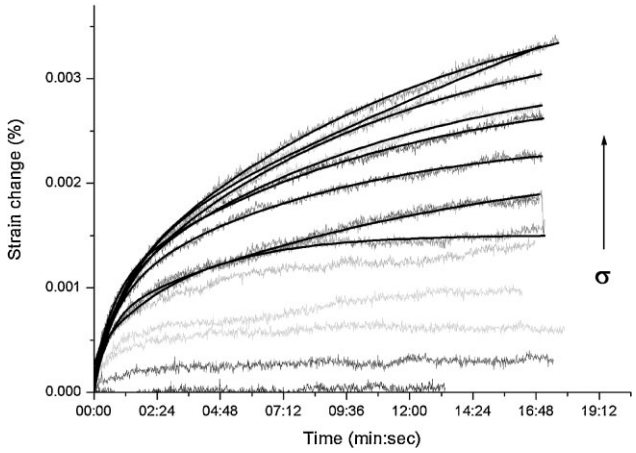

Fig. 6. The time dependence of the strain change at constant stress as a function of the applied stress for the β-eucryptite sample upon loading.

observed in β-eucryptite is contained in the first 5 min of exposure at constant stress (see below). This implies that most probably SiC is indeed more insensitive to this phenomenon, due to the absence of microcracking in its microstructure. As a reference, the SiC baseline is indicated in Figure 5 as coincident to zero strain change.

Strain–Time Dependence at Constant Stress

Another interesting feature of Figure 2, which is not immediately visible, is that the ''creep'' during each stress plateau occurs gradually, with a particular time dependence of exponential type. The dependencies of the deformation on exposure time at constant stress for the β-eucryptite sample during load are shown in Figure 6.

The attempt to fit those curves with only a single exponential function was unsuccessful. On the other hand, the curves could be well fitted with a double-exponential function, i.e.:

$$\varepsilon(t) = \varepsilon_0 + A_1\left(1 - e^{-t/T_1}\right) + A_2\left(1 - e^{-t/T_2}\right) \quad (3)$$

It was possible to obtain such a fit only at high applied stresses during loading, and no fits were possible upon unloading, i.e., the time profiles were noisy and basically flat.

The fit parameters introduced in Equation (3) also depend on applied stress. This is shown in Figure 7. We can speculate that the creep behavior observed in Figures 5 and 6 is therefore rather a relaxation phenomenon, whereby the strain adjusts itself according to microstructural rearrangements: the two relaxation mechanisms are related to changes in pore structure and in microcrack distribution. Those two relaxation processes contribute unevenly to the deformation change: the importance (amplitude, A) of the first relaxation seems to be an order of magnitude higher than the second and so seems to hold for the relaxation time T_i ($i = 1, 2$) The relaxation times grow as a function of the applied stress for both processes, but only the amplitude of the most important process (A_1) grows with applied stress. This implies that the

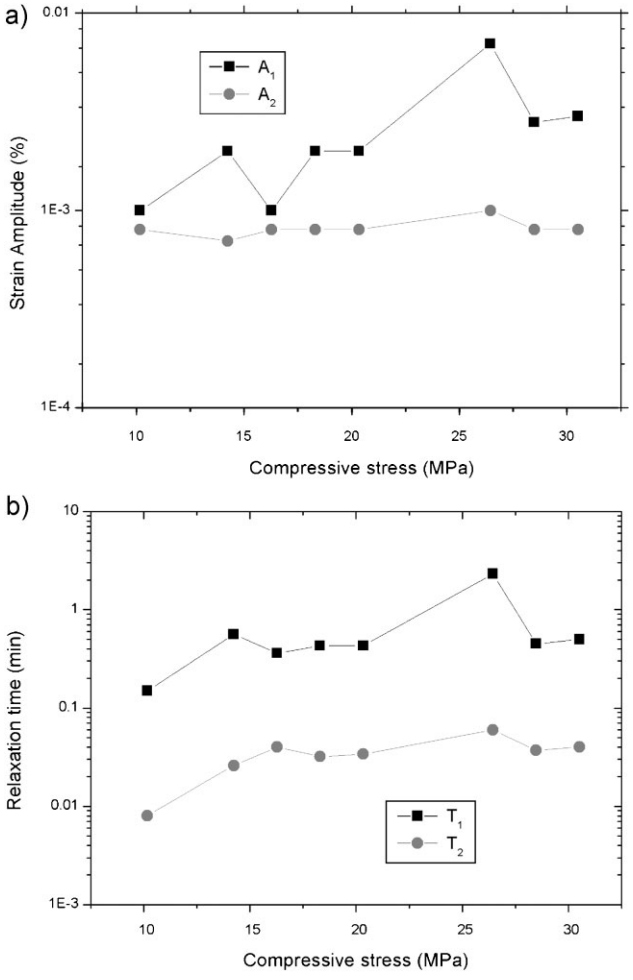

Fig. 7. The dependence of the relaxation fit parameters (a) strain amplitude, A and (b) relaxation time, T, on the applied stress for β-eucryptite upon loading.

faster phenomenon does not increase its importance as a function of the external stress, but it becomes slower, while the slower phenomenon also become slower, but contributes more heavily to the strain change.

Discussion

The industrial ceramics have very complex microstructure—they are porous and, possibly, microcracked. This complexity is manifested in the peculiar stress–strain curves shown above, resulting in a particular dependence of the elastic properties of a material on applied stress. The hysteresis area of the macroscopic stress–strain curves (Fig. 2) implies dissipation of mechanical energy at microscale, which is related to the mechanical work done during the load–unload cycle. Thus, energy dissipation is significant for β-eucryptite and negligible for SiC.

If we compare the strain scale in Figures 2 and 3, we can see the strain magnitudes are much bigger for the macroscopic than for the microscopic deformation. This means that the elastic deformation of grains represents only a part of the total

deformation. Moreover, the change of macroscopic deformation (for β-eucryptite) with stress is almost reversible—it is compressive under applied compressive load and tensile upon unload. This reversibility indicates a sponge-like stress–strain response of the β-eucryptite material: during compression, the structure accommodates the load by a macroscopic deformation of the whole body, and upon unloading the structure relaxes to the initial or close to initial state. It must be borne in mind that the residual macrostrain observed in Figure 2 could also be due to the faster stress rates and smaller number of dwells upon unloading; indeed, Figure 3(a) and 3(b) barely shows any microresidual strain at the end of the cycles.

The basic qualitative difference between two materials studied is the amount of microcracks. While microcracks are the most significant feature of the β-eucryptite microstructure (the anisotropic thermal expansion creates stresses, which are relaxed by microcracking[16,17]), they are almost undetectable in SiC (Private communication).

We can therefore explain the non-trivial dependence of Young's modulus on applied stress for β-eucryptite, since it reflects changes in the sample microstructure. It was shown that E can increase under load because of a strengthening effect due to the microcrack closure.[18] On the other hand, a softening effect because of microcrack formation (opening) seems to occur at higher loads. While classically the structure softening occurs upon cooling from the firing temperature, in our case the applied load drives this phenomenon. Thus, β-eucryptite shows the coexistence of the two processes: for low applied load microcracks start closing and the Young's modulus increases; if we further increase the load, damage takes over and E decreases to values close to the initial. Since the cracks perpendicular to the applied stress tend to close, while those parallel to the stress tend to open,[16] the microcrack dynamics of β-eucryptite on loading can be thought as sketched in Figure 8. An additional possible evidence of microcrack creation comes from Figure 3(a), where the dependence of lattice parameters a and c on stress for β-eucryptite seems to show a kink towards each other. This kink could correspond to the release of grain microstresses.

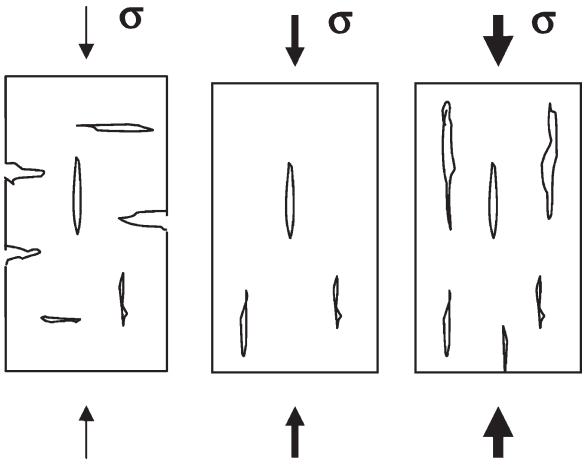

Fig. 8. The possible schematic microstructure development in β-eucryptite under load.

Upon unloading, the perpendicular microcracks re-open. This diminishes E, as it is in fact observed in Figure 4 just above 10 MPa applied stress. As mentioned before, only damage, i.e., structural softening, occurs for SiC that displays a monotonic decrease in Young's modulus during load and no change upon unloading. This makes a substantial difference between the thermal microcracks, generated during cooling from the firing temperature (and due to the anisotropic crystal thermal expansion) and the mechanical microcracks, generated during compression testing (and indicating damage). The latter are irreversible, while the former are reversible. This is in perfect coherence with the work of Heap *et al*.[4]. Those authors found on porous rocks that one needs to exceed any previously applied load to induce AE events. This implies that damage or microcracking only occurs in addition to the preexisting damage level, and basically mechanical microcracks do not close, unlike what happens for thermal cycling, otherwise AE would manifest itself always at the same applied stress level.

As far as the relaxation behavior is concerned, we can think that all microcracks act as dampers and therefore react to the load with a certain time delay. We can address to the two relaxation mechanisms (Eq. 3) mentioned above (Fig. 7) as being linked to the two distinct types of cracks: the thermal and mechanical microcracks. Whereas thermal cracks are presumed to be random oriented non-connected oblate voids of about the grain size, the mechanical cracks can be open to pores, much longer in size (about the distance between pores), and oriented primarily along the load axis. Thus, we can speculate that the relaxation process with bigger amplitude corresponds to the dynamics of mechanical cracks. Most probably these new mechanical cracks are being initiated at the pore surface points of high tensile stress and develop themselves in the axial direction through preexisting thermal microcracks of appropriate position and orientation. Instead, the second, faster process of lower and constant amplitude can be though as thermal microcrack relaxation. Basically, crack propagation is very fast while crack closure (healing) needs some time to be completed at each applied (constant) load.

The porosity itself also can play significant role in the microstructure dynamics. The porosity values for β-eucryptite and SiC are 50% and 38%, correspondingly, and the decrease in Young's modulus after the load–unload cycle is about 30 and 20% of the value before the load–unload cycle, correspondingly. The dynamics of pores under stress can be thought as the combination of two relaxation processes mentioned above: the pore flattening can be driven by compression stress, while the mechanical axial crack opening occurs via the Poisson's mechanism, as the pore closure for the thermal microcracks. Thus, the two processes of material stiffening by perpendicular microcrack closure and material damaging by axial microcrack formation plus pore deformation are therefore always present and competing against each other. The prevalence of one or the other depends

ADVANCED ENGINEERING MATERIALS

on the materials microstructure and propensity to cleavage. Therefore, the dependence of the Young's modulus on porosity cannot be assessed in the way it is done classically (see for example the extensive works of Pabst,[19] Roberts and Garboczi,[20] or Munro[21]).

The findings above imply that porous microcracked ceramics act as ''smart'' materials: they compress further under a compressive external load, thanks to the compliance of pores and microcracks. In the case they would be subjected to a constant strain, they would therefore gradually release their stress. This kind of extra deformation is given back if the level of damage is not significant and implies that the structure does not accumulate elastic energy, but rather dissipates it continuously. These facts make porous microcracked materials extremely attractive in functional applications such as membranes and filters, although stiffer non-microcracked materials such as SiC are attractive for their high strength.

As an outcome of this work, we can also recommend a very cautious use of quasi-static data for the simulation of stresses under operating conditions. Indeed, time plays a very important role and materials can adapt their strain to the external load or relax the load at fixed strain. Thus, new constitutive laws need to be taken into account for more proper modeling.

Conclusions

For the first time, the elastic properties of two porous cellular ceramic materials—β-eucryptite and silicon carbide—were studied as function of applied stress. It was found that for the microcracked material (β-eucryptite) the stress–strain curve has a peculiar time-dependent shape: the Young's modulus has a local maximum upon loading and reaches a minimum upon unloading. At each load dwell, there is a deformation change, which grows as a function of the applied stress. For the non-microcracked material (SiC) the Young's modulus decreases during loading while it remains constant upon unloading and no deformation change at constant load could be observed. This is consistent with a traditional behavior of damage accumulation during loading, and no further damage or crack closure upon unloading. It was also observed that in β-eucryptite the deformation changes on time at each constant load exposure, following a double exponential time dependence.

The observed phenomena are qualitatively explained by the microstructure adjustment, considering the paramount role of microcracking. Two main processes have been identified: thermal microcrack closure, with consequent stiffening of the body, and mechanical microcrack opening, with damage introduced to the material. Those processes act in competition at every load, with possible prevalence of one or the other. In addition, porosity, as well as the properties of the bulk (solid) material itself, can play significant role in elastic properties behavior.

It is concluded that porous microcracked ceramics act as smart materials, changing their elastic properties and their microstructure as a function of the applied load in such a way as to release their internal stress and comply with operating conditions.

The results obtained should be taken into account while modeling the life performance of industrial ceramics, since under stationary conditions (constant applied stress) they can show time-dependent behavior.

Received: June 29, 2009
Revised Version: July 6, 2009
Published online: XX XX XX

[1] E. T. Brown, J. W. Bray, F. J. Santarelli, *J. Rock Mech. Rock Eng.* **1989**, *22*, 189.
[2] S. Yu, P. Dakoulas, *J. Geotech. Eng.* **1993**, *119*, 1568.
[3] J. S. Forrester, E. H. Kisi, *J. Eur. Ceram. Soc.* **2004**, *24*, 595.
[4] M. J. Heap, S. Vinciguerra, P. G. Meredith, *Tectonophysics* **2009**, *471*, 153.
[5] M. Scalerandi, M. Nobili, M. Griffa, A. S. Gliozzi, F. Bosia, *Phys. Rev. B* **2006**, *73*, 092103.
[6] V. O. Vakhnenko, O. O. Vakhnenko, J. A. TenCate, T. J. Shankland, *Phys. Rev. B* **2007**, *76*, 184108.
[7] ASTM standard C623-92 *Standard test method for Young's modulus, Shear Modulus, and Poisson's ratio for Glass and Glass-Ceramics by Resonance*, **2000**.
[8] E. Schreiber, O. L. Anderson, N. Soga, *Elastic Constants and their Measurement*, McGraw-Hill, New York **1973**.
[9] M. A. M. Bourke, D. C. Dunand, E. Ustundag, *Appl. Phys.* **2002**, *A74*, S1707.
[10] D. J. Hughes, G. Bruno, T. Pirling, P. J. Withers, *Neutron News* **2006**, *17*, 28.
[11] T. Pirling, G. Bruno, P. J. Withers, *Mater. Sci. Eng.* **2006**, *A437*, 139.
[12] D. K. S. Chen, *ASME Winter Annual Meeting*, Dallas, Texas, **1990**.
[13] A. C. Larson, R. B. Von Dreele, *LANL Report LAUR* **2004**, *86*.
[14] T. J. Lu, N. A. Fleck, *Acta Mater.* **1998**, *46*, 4755.
[15] L. Mingshuang, L. Yulong, X. Fei, X. Zejian, C. Laifei, *Mater. Sci. Eng.* **2008**, *A489*, 120.
[16] W. R. Buessem, N. R. Thielke, R. V. Sarakauskas, *Ceram. Age* **1952**, *60*, 38.
[17] A. M. Efremov, *Phil. Mag.* **2006**, *86*, 5431.
[18] M. L. Batzle, G. Simmons, R. W. Siegfried, *J. Geophys. Res.* **1980**, *85*, 7072.
[19] W. Pabst, E. Gregorova, *J. Mater. Sci.* **2004**, *39*, 3501.
[20] A. P. Roberts, E. J. Garboczi, *J. Am. Ceram. Soc.* **2000**, *83*, 3041.
[21] R. G. Munro, *J. Res. Nat. Bur. Stand.* **2004**, *109*, 497.

